Topological phases in spin-orbit coupled dipolar lattice bosons

H. T. Ng
Center for Quantum Information, Institute for Interdisciplinary Information Sciences, Tsinghua University, Beijing 100084, P. R. China

(Dated: December 2, 2014)

We study the topological phases in spin-orbit coupled dipolar bosons in a one-dimensional optical lattice. The magnetic dipolar interactions between atoms give rise to the inter-site interactions. In the Mott-insulating regime, this system can be described by the quantum XYZ spin model with the Dzyaloshinskii-Moriya interactions in a transverse field. We focus on investigating the effect of dipolar interactions on the topological phase. The topological phase can be shown when spin-orbit coupling incorporates with the repulsive dipolar interaction. We find that the dipolar interaction can broaden the range of parameters of spin-orbit coupling and transverse field for exhibiting the topological phase. The sum of spin correlations between the two nearest neighbouring atoms can be used to indicate the topological phase. This may be useful for detecting topological phases in experiments.

PACS numbers: 03.75.Mn, 37.10.Jk, 67.85.Hj

I. INTRODUCTION

Majorana fermions are exotic particles, where their anti-particles are their own particles [1]. Since Kitaev [2] found that an unbound pair of Majorana fermions can be realized in a one-dimensional (1D) spin-polarized superconductor, a considerable effort has been devoted to studying semiconducting wires [3, 4] and cold atoms in optical lattices [5, 6] for realization of Majorana fermions. In addition, Majorana fermions are robust against local perturbations due to the topological degeneracy. Therefore, it may be potentially applied to quantum information processing such as quantum memory [7] and topological quantum computing [8, 9].

Ultracold atoms have been used for simulating various quantum many-body phenomena [10]. For example, quantum phase transition from a superfluid to a Mott insulator [11] has been shown in lattice bosons. Also, spin-orbit (SO) coupling in a Bose-Einstein condensate (BEC) has been shown in an experiment [12], where the two atomic spin states are coupled to their momentum states by using a pair of lasers. In fact, SO coupling is essential to realize topological matter [13, 14]. Therefore, ultracold atoms pave the way for studying topological phases [15].

Recently, SO-coupled dipolar condensates have been theoretically studied [16, 17]. The intriguing ground state of ultracold atoms can be displayed via the interplay of SO coupling and magnetic dipole-dipole interaction (DDI). Indeed, dipolar interactions in ultracold atomic gases can give rise to spectacular quantum phenomena [18] such as spin texture [19] and Einstein-de Haas effect [20]. In addition, a chromium gas in an optical lattice [21, 22] has recently been realized. Since a chromium atom has a relatively large magnetic dipole moment [23], the inter-site interactions become strong enough [22] to experimentally study quantum magnetism [24].

In this paper, we consider spin-orbit coupled bosonic atoms in a 1D optical lattice, where the atoms at the different sites couple to each other via the magnetic dipolar interactions [22]. In the Mott-insulating regime, this system can be described by the quantum XYZ spin model with the Dzyaloshinskii-Moriya (DM) interactions in a transverse field [25–27], where a two-component boson in each site can be viewed as a spin-half particle [28]. Indeed, a spin chain is equivalent to a 1D spinless fermion model by performing the Jordan-Wigner transformation [29]. This enables us to study the topological phenomenon, such as Majorana fermions, with a quantum spin chain [29, 30].

The long-ranged DDI leads to interactions between the two atoms at the different sites. It is important to examine the effect of long-ranged interactions on the topological phases [31–35]. Although the magnetic dipolar interactions between the atoms are weak, such strengths are comparable to effective coupling strengths between the spins [22] in the Mott-insulating regime. Therefore, *the effect of SO coupling, DDI and transverse field on the topological phases can be studied in a controllable manner.*

Here we study the energy difference between two degenerate ground states in the two different parity sectors to determine the topological phase [31]. When the energy difference becomes zero, the topological degeneracy occurs in the system. Although the DM interactions break the $\mathbb{Z}_2$ symmetry in this system [29], the system exhibits the topological phase if the DM interactions are sufficiently small. We find that the SO couplingz incorporate with repulsive DDIz can be used to exhibit topological phases. A topological phase is shown when the SO coupling strength increases with the dipolar interaction strength. Also, the DDI can broaden the range of SO coupling and transverse field strengths for exhibiting topological phases. Therefore, this may lead to observing topological phases in 1D SO-coupled dipolar lattice bosons.

In addition, we show that the sum of all spin-polarization correlations between nearest neighbouring

atoms can be used for characterizing the magnetic properties of a spin chain. When the system is in a topological phase, the sum of spin correlations is close to zero. This coincides with the topological phase which is determined by using the energy gap between the two different parity sectors. In fact, spin correlations between the spins in the different sites have been probed in a 1D optical lattice [36]. Thus, this can be used for detecting the topological phases in experiments.

This paper is organized as follows: In Sec. II, we introduce the system of SO-coupled dipolar bosons in a 1D lattice. In Sec. III, we discuss the system in the Mott-insulating regime. In Sec. IV, we study the effect of dipolar interactions and the transverse field on topological phases. We provide a summary in Sec. V.

II. SYSTEM

We consider the two-component dipolar bosonic atoms to be trapped a 1D optical lattice, where the atoms are spin-orbit coupled [12]. Recently, a spin-orbit coupled dipolar condensate has recently been discussed [16, 17], where the two internal states can be chosen in the ground electronic manifold [16] for SO coupling. In this system, the atoms interact with each other via short-range and long-range interactions, and the two neighbouring atoms are coupled through SO coupling. The total system can be described by a Hamiltonian:

$$H = H_{\rm BH} + H_{\rm SO} + H_d, \tag{1}$$

where $H_{\rm BH}$ describes the tunnel coupling and short-range atom-atom interactions, and $H_{\rm SO}$ and H_d describe the SO couplings and magnetic DDIs between the atoms, respectively.

Let us describe this system in more detail. The two-component Bose-Hubbard model can be used to describe the interactions of two-component bosons in an optical lattice. We consider this system to have open boundary conditions. The Hamiltonian $H_{\rm BH}$ can be written as, ($\hbar = 1$),

$$H_{\rm BH} = \sum_{\alpha,i} \Big[\epsilon_i^\alpha n_i^\alpha + J_\alpha(\alpha_i^\dagger \alpha_{i+1} + \text{H.c.}) + \frac{U_\alpha}{2} n_i^\alpha (n_i^\alpha - 1) + U_{ab} n_i^a n_i^b\Big], \tag{2}$$

where α_i and $\alpha_i^\dagger$ are the annihilation and creation operators of a single atom in the state $|\alpha\rangle$, and n_i^α is the number operator at site i, and $\alpha = a, b$. The parameter ϵ_i^α is the strength of harmonic confinement at site i, J_α is the tunnel coupling, $U_{a(b)}$ and U_{ab} are atomic interaction strengths of the intra- and inter-component of atoms, respectively. For simplicity, we consider the tunnel coupling and atom-atom interaction strength of each component to be nearly equal, i.e., $J_a \approx J_b \approx J$ and $U_a \approx U_b \approx U$. We assume that the atoms in each component are additionally trapped in a very shallow harmonic potential, and therefore $\epsilon_i^\alpha \approx \epsilon^\alpha$ are roughly equal to each other.

Spin-orbit coupling can be generated by inducing two-photon Raman transition using a pair of lasers [12]. By choosing the appropriate phases of lasers, the opposite spin states of atoms at two neighbouring sites can be coupled [37]. Alternatively, the method for generating SO coupling without using near resonant light has also been proposed [38]. The Hamiltonian, which describes SO coupling between two sites, can be written as [37, 39]

$$H_{\rm SO} = t_{so} \sum_i (a_i^\dagger b_{i+1} - a_i^\dagger b_{i-1} + \text{H.c.}), \tag{3}$$

where t_{so} is the strength of spin-orbit coupling.

We consider the atoms to interact with each other due to their magnetic dipoles. We consider the relative position of two magnetic dipoles to be $\vec{r}$. The DDI energy between the two atoms is given by [40]

$$U_{dd}(r) = \frac{C_{dd}}{4\pi} \frac{(\mathbf{S}_1 \cdot \mathbf{S}_2) - 3(\mathbf{S}_1 \cdot \vec{r})(\mathbf{S}_2 \cdot \vec{r})}{r^3}, \tag{4}$$

where $C_{dd} = \mu_0 (g\mu_B)^2$ is the dipolar interaction strength. The parameters μ_0, g and μ_B are the magnetic permeability of vacuum, the Lande factor, and the Bohr magneton, respectively. Here $\mathbf{S}_i$ is the angular momentum operator of the two spin states of atoms.

We consider the dipolar interactions which conserve the angular momentum of internal spin states between the different sites. Indeed, the dipolar interactions also lead to the transition between the different spin states with accompanying the change of orbital angular momentum. By applying a sufficiently small magnetic field, the non-conserving terms of atomic spin states can be neglected [22] due to the large energy difference between the change of magnetic energy and the potential depth in the lattice [21].

III. MOTT-INSULATING REGIME

We discuss the bosonic lattice in the strong atom-atom interaction regime, and the lattice is at unit filling. We assume that the atom-atom interaction strengths U and U_{ab} are repulsive. We consider the atomic interaction strengths U and U_{ab} to be much larger than the parameters such as J, t_{so} and $|\epsilon^b - \epsilon^a|$. In this strongly interacting regime, a single atom is allowed to occupy in each potential well. We have the four degenerate states for the two neighbouring sites, i.e., $|1_i^a, 0_i^b\rangle|0_{i+1}^a, 1_{i+1}^b\rangle$, $|1_i^a, 0_i^b\rangle|1_{i+1}^a, 0_{i+1}^b\rangle$, $|0_i^a, 1_i^b\rangle|0_{i+1}^a, 1_{i+1}^b\rangle$ and $|0_i^a, 1_i^b\rangle|1_{i+1}^a, 0_{i+1}^b\rangle$. In this case, the two-mode bosonic operators can be written in terms of angular momentum operators, i.e., $S_i^+ = a_i^\dagger b_i$, $S_i^- = b_i^\dagger a_i$ and $S_i^z = (b_i^\dagger b_i - a_i^\dagger a_i)/2$. By using the second-order perturbation theory, the effective Hamiltonian, describes the

tunnel and spin-orbit couplings, is written as [26, 27]

$$H^s_{\rm eff} = \lambda \sum_{i=1}^{N-1} \Big\{ \frac{\Delta}{\lambda} S^z_i + 2\Big[\Big(\frac{t_{so}}{J}\Big)^2 - 1\Big]\Big(2\frac{U_{ab}}{U} - 1\Big) S^z_i S^z_{i+1} + \Big(\frac{t_{so}}{J}\Big)^2 (S^+_i S^+_{i+1} + S^-_i S^-_{i+1}) - (S^+_i S^-_{i+1} + S^-_i S^+_{i+1}) - 4\frac{U_{ab}}{U}\Big(\frac{t_{so}}{J}\Big)(S^z_i S^x_{i+1} - S^x_i S^z_{i+1})\Big\} \quad (5)$$

where $\lambda = 2J^2/U_{ab}$ and $\Delta = \epsilon^b - \epsilon^a$. The last terms in Eq. (5) are known as the DM interactions [26, 27]. Therefore, this model can be mapped onto the XYZ spin model with the DM interactions in a transverse field.

In addition, the Hamiltonian, describes the dipolar interactions, can be written as [22]

$$H_d = \sum_{i,j} \eta_{ij} \Big[S^z_i S^z_j - \frac{1}{4}(S^+_i S^-_j + S^-_i S^+_j)\Big], \quad (6)$$

where η_{ij} is the dipolar interaction strength between site i and j. The parameter η_{ij} can be approximated [18] by $C_{dd}(1 - 3z^2_{ij}/r^2_{ij})/4\pi r^3_{ij}$ being multiplied by the number densities of the two local sites, where r_{ij} is the relative position between two dipoles at sites i and j and z is the z-component of r_{ij}. The Hamiltonian H_d describes the Heisenberg interactions in the spin model [40]. We will consider the atoms to interact with their nearest neighbours with the dipolar interaction strength η_1. Here the dipolar interaction strengths are comparable to the effective coupling strengths in Eq. (5) which is derived from the second-order perturbation theory.

IV. TOPOLOGICAL PHASE

Since the spin model has the $\mathbb{Z}_2$ symmetry, the parity number P is preserved, where P is defined as [29]

$$P = \prod_{i=1}^{N} \sigma^z_i. \quad (7)$$

In this model, there are two parity sectors which are called even ($P = 1$) and odd ($P = -1$) parities, respectively.

We consider the energy difference between the two ground states in the odd and even parities to indicate the topological phase of a spin chain [31]. It is defined as

$$\Delta E = |E_{\rm odd} - E_{\rm even}|, \quad (8)$$

where $E_{\rm odd}$ and $E_{\rm even}$ are the ground-state energies of the odd- and even-parity sectors. The system is in a topological phase if the energy difference ΔE between two different parity sectors is zero. Thus, ΔE can act as an order parameter for topological phases.

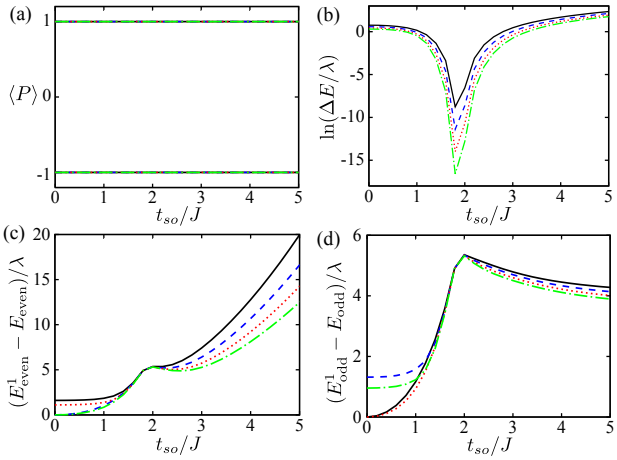

FIG. 1. (Color online) In (a), the expectation of parities $\langle P \rangle$ of the two degenerate ground states are plotted. In (b), logarithmic scale of the energy gap ΔE are plotted versus spin-orbit coupling strength t_{so}, for the different Ns. The energy difference between the first excited and ground states in the even and odd parities are plotted in (c) and (d), respectively. The different number of atoms N are denoted by the different lines: $N = 8$ (black solid), $N = 10$ (blue dashed), $N = 12$ (red dotted) and $N = 14$ (green dash-dotted). The nearest neighbour dipolar interaction strength η_1 is equal to 5λ and $U_{ab}/U = 0.25$.

A. Effect of dipolar interactions

We study the relationship between spin-orbit couplings and dipolar interactions to the topological degeneracy. We numerically solve the eigen-energy by using exact diagonalization method. It should be noted that the DM terms in Eq. (5) break the $\mathbb{Z}_2$ symmetry. We plot the parities of the two degenerate ground states in Fig. 1(a). When the ratio U_{ab}/U of the inter- and intra-component interactions is smaller than one, this system exhibits the two definite parities 1 and -1 in Fig. 1(a), respectively. This means that the two degenerate ground states preserve their parities if the DM terms are small enough. To show the topological degeneracy, we study the energy gap ΔE in Eq. (8) versus the SO coupling in Fig. 1(b), for the different sizes of system. The energy splitting decreases exponentially when the size N grows. This shows the feature of the topological degeneracy [29].

We also plot the energy difference between the first excited and ground states for the even- and odd-parity sectors in Fig. 1(c) and (d), respectively. The energy gaps are shown in the different parities, where they are much larger than the energy splitting between the two nearly degenerate states. Therefore, the two degenerate ground states can be protected by the energy gaps.

In Fig. 2, we plot the contour plot of $\ln(\Delta E)$ versus the dipolar interaction and spin-orbit coupling strengths, for the different ratios of U_{ab}/U. The blue area is shown when the SOC strength increases with the repulsive dipolar interaction strength. This blue area denotes that the

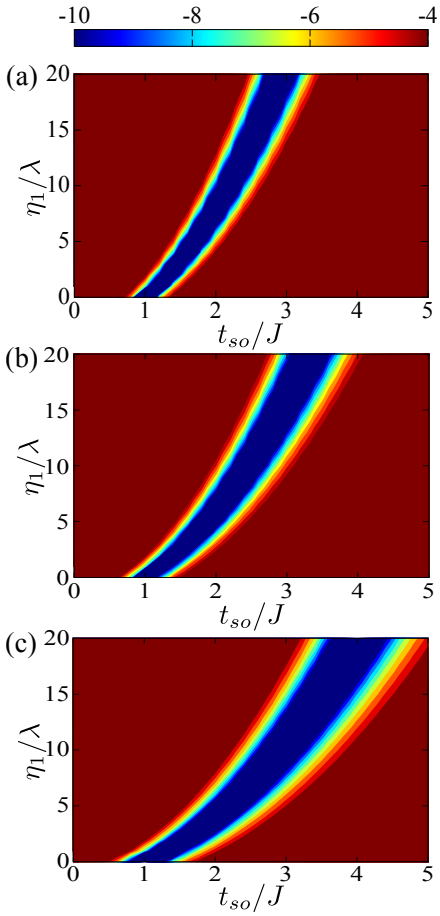

FIG. 2. (Color online) Contour plot of $\ln(\Delta E/\lambda)$ versus dipolar interaction η_1 and spin-orbit coupling strength t_{so}, for $N = 14$. The different ratios of U_{ab}/U are shown: (a) $U_{ab}/U = 0$, (b) $U_{ab}/U = 0.25$ and (c) $U_{ab}/U = 0.5$.

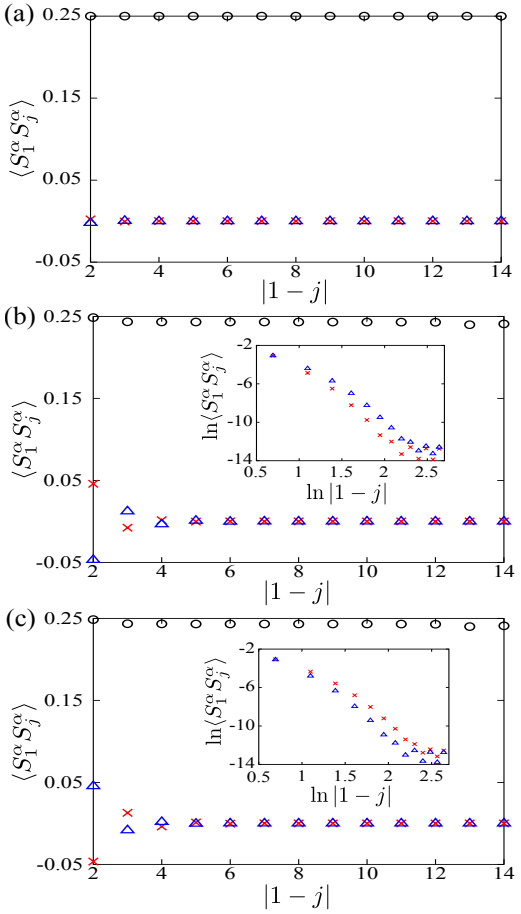

FIG. 3. (Color online) Spin correlations versus $|1-j|$, for $N = 14$ and $U_{ab}/U = 0.5$. $\langle S_1^x S_j^x \rangle$, $\langle S_1^y S_j^y \rangle$ and $\langle S_1^z S_j^z \rangle$ are denoted by red upper-triangle, black circle and blue cross, respectively. The different of SO couling strengths are shown: (a) $t_{so} = 2.9J$, (b) $t_{so} = 2.6J$ and (c) $t_{so} = 3.3J$. The two insets in (b) and (c) show the log-log plots of spin correlations $\langle S_1^x S_j^x \rangle$ and $\langle S_1^z S_j^z \rangle$ versus the distance $|1-j|$.

energy difference ΔE is below 1×10^{-4}. In addition, the blue region becomes larger when the dipolar interaction strength increases as shown in Fig. 2. This result suggests that the repulsive dipolar interactions can widen the range of SO coupling strengths for exhibiting the topological phases.

Indeed, the topological phase can be described by the ground states of the Ising model along the y-direction. When $t_{so} = J$ and $U_{ab}/U = 0$, the Hamiltonian $H^s_{\rm eff}$ in Eq. (5) can be reduced to $-4\lambda \sum_i S_i^y S_{i+1}^y$. The two degenerate ground states are $|\uparrow\uparrow \ldots \uparrow\rangle_y$ and $|\downarrow\downarrow \ldots \downarrow\rangle_y$, where $|\uparrow\rangle_j$ and $|\downarrow\rangle_j$ are spin up and down states in the y-direction at site j. "Tunneling" between these two ground states occurs due to the virtual transitions via the other perturbation terms in the Hamiltonian [29]. Therefore, it falls off exponentially with the size N as shown in Fig. 1(b). When the dipolar interaction increases and U_{ab}/U is smaller than one, the topological phase can still be described in this picture, i.e., the terms $-\sum_i S_i^y S_{i+1}^y$ are dominant. This can be manifested in studying the spin correlations.

In Fig. 3(a), we plot the spin correlations $\langle S_1^y S_j^y \rangle$ versus the distance $|1-j|$, where $U_{ab}/U = 0.5$, $t_{so} = 2.9J$ and $\alpha = x, y, z$. Spin correlations $\langle S_1^y S_j^y \rangle$ are equal to 0.25 and do not decay between the distant spins, while $\langle S_1^x S_j^x \rangle$ and $\langle S_1^z S_j^z \rangle$ almost vanish. We also study the spin correlations near the boundary of topological phase, where $t_{so} = 2.6J$ and $3.3J$. In Figs. 3(b) and (c), $\langle S_1^y S_j^y \rangle$ is slightly smaller than 0.25 and $\langle S_1^x S_j^x \rangle$ and $\langle S_1^z S_j^z \rangle$ decay algebraically in both cases. Therefore, the system starts to show the feature of the incomplete ferromagnet phase [26].

Next, we study the spin correlations of the two degenerate ground states. We introduce a parameter S which is defined as

$$S = \sum_{i=1}^{N-1} \langle S_i^z S_{i+1}^z \rangle. \tag{9}$$

If two spins are in parallel, then the spin correlation $\langle S_i^z S_{i+1}^z \rangle$ will be positive. Otherwise, the two spins are

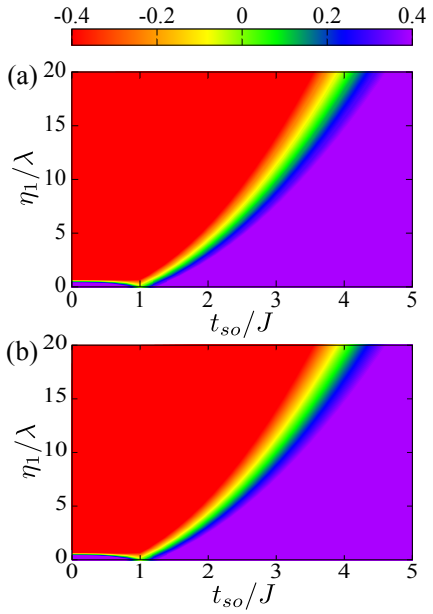

FIG. 4. (Color online) Contour plots of parameter S versus dipolar interaction η_1 and spin-orbit coupling strength t_{so}, for $N = 14$ and $U_{ab}/U = 0.5$. The ground states in even- and odd-parity are shown in (a) and (b), respectively.

anti-parallel if $\langle S_i^z S_{i+1}^z \rangle$ is negative. When S is positive(negative), there is a higher probability to find the two nearest spins in parallel(anti-parallel). If S becomes zero, then there is an equal probability of finding the two spins in parallel or anti-parallel. Since the topological phase can be described by the degenerate states $|\uparrow\uparrow \ldots \uparrow\rangle_y$ and $|\downarrow\downarrow \ldots \downarrow\rangle_y$, the parameter S becomes zero. Thus, this parameter S can thus be used to indicate the topological phase as long as U_{ab}/U is smaller than one.

In Fig. 4, we plot the contour plots of S versus the dipolar interaction and SO coupling for the two ground states in the even- and odd-parity in (a) and (b), respectively. It is corresponding to Fig. 2(c), where U_{ab}/U is equal to 0.5. In Fig. 4(a) and (b), the left part is red ($S > 0$) and the right part is purple ($S < 0$). The small region, which gives $S \approx 0$, is in between these two different regions. This region ($S \approx 0$) coincides the region which shows topological degeneracy in Fig. 2(c). Therefore, the parameter S can be used for detecting the topological phases.

B. Effect of transverse field in the presence of dipolar interactions

We study the effect of the transverse field on topological degeneracy in the presence of repulsive DDIs. In Fig. 5, the logarithmic scale of ΔE are plotted versus the transverse field and SO coupling, for the different dipolar interaction strengths. The stronger dipolar interaction strength are shown from Fig. 5(a) to (c). We can see that the blue area becomes larger when the dipolar interactions are stronger. This means that the topological degeneracy can be obtained from a wider range of parameters Δ and t_{so} when the dipolar interaction strength increases. The repulsive dipolar interactions are therefore useful to exhibit the topological phases.

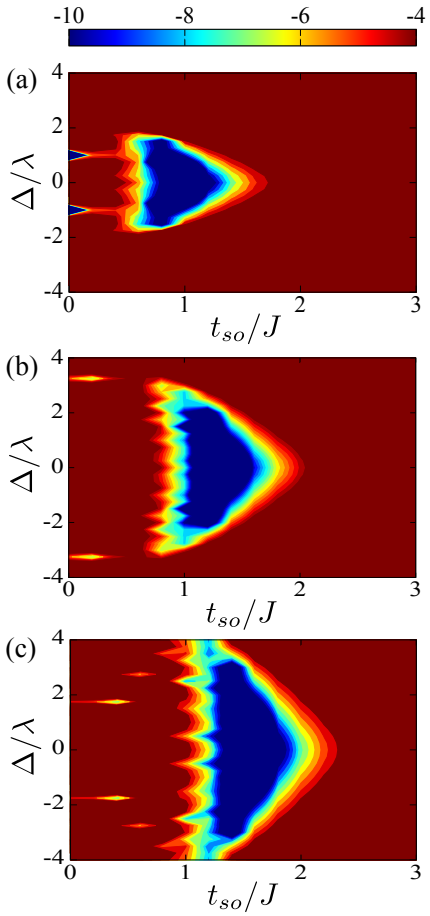

FIG. 5. (Color online) Contour plots of $\ln(\Delta E/\lambda)$ versus transverse field strength Δ and spin-orbit coupling strength t_{so} , for $N = 14$ and $U_{ab}/U = 0.5$. The different strengths of dipolar interaction η_1 are plotted in (a) $\eta_1 = 0$, (b) $\eta_1 = \lambda$ and (c) $\eta_1 = 2\lambda$, respectively.

Then, we investigate the parameter S in Eq. (9) for indicating the topological phase. In Fig. 6, the contour plots of the parameter S are shown versus the transverse field and SO coupling, for the even- and odd-parity in (a) and (b), respectively and $\eta_1 = 2\lambda$. The half of an ellipse is shown to be red when the parameter S is negative. The outside region is purple where S is positive. The boundary of the red half ellipse indicates S to be equal to zero. To compare figures 5(c) and 6, this small region coincides with the blue area which shows the topological degeneracy in Fig. 5(c). Therefore, the parameter S is an useful parameter to indicate the topological phase.

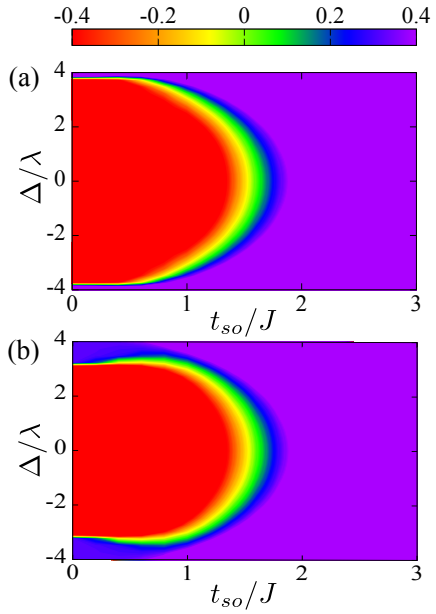

FIG. 6. (Color online) Contour plots of parameter S versus transverse field strength Δ and spin-orbit coupling strength t_{so}, for $N = 14$, $U_{ab}/U = 0.5$ and $\eta_1 = 2\lambda$. The ground states in even- and odd-parity are shown in (a) and (b), respectively.

V. DISCUSSION

Let us estimate the physical parameters for observing the topological phase. It should be noted that the ratio J/U can be tuned in experiments. As demonstrated in the experiment [41], the superexachange interaction strength $2\lambda = 4J^2/U_{ab}$ can be adjusted to about 5 Hz with a high barrier depth. The dipolar coupling strength between the atoms in the nearest site is about $\sim$ 20 Hz if chromium atoms are used. This has been shown in the recent experiment [22]. Therefore, the ratio of the dipolar interaction strength η_1 ($\sim$ 20 Hz) to the superexchange interaction strength λ ($\sim$ 2 Hz) can attain ~ 10. Therefore, the effect of dipolar interactions on the topological phase can be detected with the current experimental setting.

VI. CONCLUSION

In summary, we have studied a 1D spin-orbit coupled dipolar lattice bosons, where the atoms at the different sites can be coupled via the magnetic dipolar interactions. In the Mott-insulating regime, this system can be described by the quantum XYZ model with the DM interactions in a transverse field. We adopt the energy difference between the two ground states in the different parities to determine the topological phase. The repulsive DDI can broaden the parameter range of SO coupling and transverse field strengths for exhibiting topological phases. We show that the sum of the spin polarization correlations between two nearest neighbouring atoms can be used to indicate topological phases. It may be useful to detect the topological phase in experiments.

ACKNOWLEDGMENTS

We thank Jize Zhao and Marie Piraud for useful discussion. This work was supported in part by the National Basic Research Program of China Grants No. 2011CBA00300 and No. 2011CBA00301 the National Natural Science Foundation of China Grants No. 11304178, No. 61061130540, and No. 61361136003.

[1] F. Wilczek, Nat. Phys. **5**, 614 (2009).
[2] A. Y. Kitaev, Physics-Uspekhi **44**, 131 (2001).
[3] R. M. Lutchyn, J. D. Sau and S. Das Sarma, Phys. Rev. Lett. **105**, 077001 (2010).
[4] Y. Oreg, G. Refael and F. von Oppen, Phys. Rev. Lett. **105**, 177002 (2010).
[5] C. V. Kraus, S. Diehl, P. Zoller and M. A. Baranov, New J. Phys. **14**, 113036 (2012).
[6] L. Jiang, T. Kitagawa, J. Alicea, A. R. Akhmerov, D. Pekker, G. Refael, J. I. Cirac, E. Demler, M. D. Lukin and P. Zoller, Phys. Rev. Lett. **106**, 220402 (2011).
[7] L. Mazza, M. Rizzi, M. D. Lukin, J. I. Cirac, Phys. Rev. B **88**, 205142 (2013).
[8] C. Nayak, S. H. Simon, A. Stern, M. Freedman and S. Das Sarma, Rev. Mod. Phys. **80**, 1083 (2008).
[9] J. Alicea, Y. Oreg, G. Refael, F. von Oppen and M. P. A. Fisher, Nat. Phys. **7**, 412 (2011).
[10] I. Bloch, J. Dalibard and S. Nascimbène, Nat. Phys. **8**, 267 (2012).
[11] M. Greiner, O. Mandel, T. Esslinger, T. W. Hänsch and I. Bloch, Nature **415**, 39 (2002).
[12] Y.-J. Lin, K. Jiméenz-García and I. B. Spielman, Nature **471**, 83 (2011).
[13] M. Z. Hasan and C. L. Kane, Rev. Mod. Phys. **82**, 3045 (2010).
[14] X.-L. Qi and S.-C. Zhang, Rev. Mod. Phys. **83**, 1057 (2011).
[15] V. Galitski and I. B. Spielman, Nature **494**, 49 (2013).
[16] Y. Deng, J. Cheng, H. Jing, C.-P. Sun and S. Yi, Phys. Rev. Lett. **108**, 125301 (2012).
[17] R. M. Wilson, B. M. Anderson and C. W. Clark, Phys. Rev. Lett. **111**, 185303 (2013).
[18] T Lahaye, C Menotti, L Santos, M Lewenstein and T Pfau, Rep. Prog. Phys. **72**, 126401 (2009).
[19] M. Vengalattore, S. R. Leslie, J. Guzman and D. M. Stamper-Kurn, Phys. Rev. Lett. **100**, 170403 (2008).
[20] T. Swislocki, T. Sowinski, J. Pietraszewicz, M. Brewczyk, M. Lewenstein, J. Zakrzewski and M. Gajda, Phys. Rev. A **83**, 063617 (2011).

[21] A. de Paz, A. Chotia, E. Maréchal, P. Pedri, L. Vernac, O. Gorceix, and B. Laburthe-Tolra, Phys. Rev. A 87, 051609(R) (2013).

[22] A. de Paz, A. Sharma, A. Chotia, E. Maréchal, J. H. Huckans, P. Pedri, L. Santos, O. Gorceix, L. Vernac, and B. Laburthe-Tolra, Phys. Rev. Lett. **111**, 185305 (2013).

[23] L. Santos and T. Pfau, Phys. Rev. Lett. **96**, 190404 (2006).

[24] A. Auerbach, *Interacting electrons and quantum magnetism*, (Springer, New York, 1994).

[25] X. F. Zhou, Y. Li, Z. Cai and C. J. Wu, J. Phys. B, **46** 134001 (2013).

[26] M. Piraud, Z. Cai, I. P. McCulloch, U. Schollwck, Phys. Rev. A **89**, 063618 (2014).

[27] J. Z. Zhao, S. J. Hu, J. Chang, F. W. Zheng, P. Zhang, X. Q. Wang, arXiv:1403.1316.

[28] L.-M. Duan, E. Demler and M. D. Lukin, Phys. Rev. Lett. **91**, 090402 (2003).

[29] A. Kitaev, C. Laumann, arXiv:0904.2771.

[30] A. Mezzacapo, J. Casanova, L. Lamata and E. Solano, New J. Phys. **15**, 033005 (2013).

[31] E. M. Stoudenmire, J. Alicea, O. A. Starykh, M. P. A. Fisher, Phys. Rev. B **84**, 014503 (2011).

[32] S. Gangadharaiah, B. Braunecker, P. Simon and Daniel Loss, Phys. Rev. Lett. **107**, 036801 (2011).

[33] E. Sela, A. Altland and A. Rosch, Phys. Rev. B **84**, 085114 (2011).

[34] F. Hassler and D. Schuricht, New J. Phys. **14**, 125018 (2012).

[35] R. Thomale, S. Rachel and P. Schmitteckert, Phys. Rev. B **88**, 161103(R) (2013).

[36] M. Endres, M. Cheneau, T. Fukuhara, C. Weitenberg, P. Schauss, C. Gross, L. Mazza, M.C. Banuls, L. Pollet, I. Bloch and S. Kuhr, Science **334**, 200 (2011).

[37] X.-J. Liu, Z.-X. Liu and M. Cheng, Phys. Rev. Lett. **110**, 076401 (2013).

[38] C. J. Kennedy, G. A. Siviloglou, H. Miyake, W. C. Burton and W. Ketterle, Phys. Rev. Lett. **111**, 225301 (2013).

[39] Z. Cai, X. Zhou and C. Wu, Phys. Rev. A **85**, 061605(R) (2012).

[40] S. Hensler *et al.*, Appl. Phys. B **77**, 765 (2003).

[41] S. Trotzky, P. Cheinet, S. Fölling, M. Feld, U. Schnorrberger, A. M. Rey, A. Polkovnikov, E. A. Demler, M. D. Lukin and I. Bloch, Science **319**, 295 (2008).